Astronomy & Astrophysics manuscript no. ska November 3, 2008
(DOI: will be inserted by hand later)

Pulsar searches and timing with the SKA

R. Smits[1], M. Kramer[1], B. Stappers[1], D.R. Lorimer[2,3], J. Cordes[4], and A. Faulkner[1]

[1] Jodrell Bank Centre for Astrophysics, University of Manchester
[2] Department of Physics, 210 Hodges Hall, West Virginia University, Morgantown, WV 26506, USA
[3] National Radio Astronomy Observatory, Green Bank
[4] Astronomy Department, Cornell University, Ithaca, NY

Received date / Accepted date

Abstract. The Square Kilometre Array (SKA) is a planned multi purpose radio telescope with a collecting area approaching 1 million square metres. One of the key science objectives of the SKA is to provide exquisite strong-field tests of gravitational physics by finding and timing pulsars in extreme binary systems such as a pulsar-black hole binary. To find out how three preliminary SKA configurations will affect a pulsar survey, we have simulated SKA pulsar surveys for each configuration. We estimate that the total number of normal pulsars the SKA will detect, using only the 1-km core and 30 minutes integration time, is around 14 000 normal pulsar and 6 000 millisecond pulsars. We describe a simple strategy for follow-up timing observations and find that, depending on the configuration, it would take 1–6 days to obtain a single timing point for 14 000 pulsars. Obtaining a single timing point for the high-precision timing projects of the SKA, will take less than 14 hours, 2 days, or 3 days, depending on the configuration. The presence of aperture arrays will be of great benefit here. We also study the computational requirements for beam forming and data analysis for a pulsar survey. Beam forming of the full field of view of the single-pixel feed 15-m dishes using the 1-km core of the SKA requires about 2.2×10^{15} operations per second. The corresponding data rate from such a pulsar survey is about 4.7×10^{11} bytes per second. The required computational power for a deep real time analysis is estimated to be 1.2×10^{16} operations per second. For an aperture array or dishes equipped with phased array feeds, the survey can be performed faster, but the computational requirements and data rates will go up.

Key words. Stars: neutron – (Stars:) pulsars: general – Telescopes

1. Introduction

There are, arguably, no other astronomical objects whose discovery and subsequent studies provides more insight in such a rich variety of physics and astrophysics than radio pulsars. Pulsars find their applications (see e.g. Lorimer & Kramer 2005) in the study of the Milky Way, globular clusters, the evolution and collapse of massive stars, the formation and evolution of binary systems, the properties of super-dense matter, extreme plasma physics, tests of theories of gravity, the detection of gravitational waves, and astrometry, to name only a few areas. Indeed, many of these areas of fundamental physics can be best – or even only – studied, using radio observations of pulsars.

To harvest the copious amount of information and science accessible with pulsars, two different types of observations are required. Firstly, suitable pulsars need to be discovered via radio surveys that sample the sky with high time and frequency resolution. Depending on the particular region of sky to be covered (e.g. along the Galactic plane vs. higher Galactic latitudes), different technical requirements may be needed. Secondly, after the discovery, a much larger amount of observing is required to extract most of the science using pulsar timing observations, i.e. the regular high-precision monitoring of the pulse times-of-arrival and the pulse properties. Again, depending on the type of sources to be monitored (e.g. young pulsars in supernova remnants vs. millisecond pulsars in Globular clusters) the requirements are different.

In the past 40 years, astronomers have impressively demonstrated the potential of pulsar search and timing observations (e.g. Hulse & Taylor 1975). However, the next 10-15 years promise to revolutionise pulsar astrophysics in a way that is without parallel in the history of pulsars or radio astronomy in general. This revolution will be provided by the next generation radio telescope known as the "Square-Kilometre-Array" (SKA) (e.g. Terzian & Lazio 2006). The SKA will be the largest telescope ever built, with a maximum baseline of 3 000+ km and about a factor of 10–100 more powerful (both in sensitivity and survey

Send offprint requests to: R. Smits e-mail: Roy.Smits@manchester.ac.uk

speed) than any other radio telescope. The SKA will be particularly useful for pulsars and their applications in astrophysics and fundamental physics. Due to the large sensitivity of the SKA, not only a Galactic census of pulsars can be performed, but the discovered pulsars can also be timed more precisely than before. As a result, the pulsar science enabled by the SKA and described by Cordes et al. (2004) and Kramer et al. (2004) includes:

- Finding rare objects that provide the greatest opportunities as physics laboratories. Examples include:
  - Binary pulsars with black hole companions, which enable strong-field tests of General Relativity.
  - Pulsars in the Galactic Centre, which will probe conditions near a $3 \times 10^6\,\mathrm{M}_\odot$ black hole.
  - Millisecond pulsars that can act in an ensemble (known as Pulsar Timing Array) as detectors of low-frequency (nHz) gravitational waves of astrophysical and cosmological origin
  - Millisecond pulsars spinning faster than 1.4 ms that can constrain the equation-of-state of super-dense matter.
  - Pulsars with translational speeds in excess of $10^3\,\mathrm{km\,s^{-1}}$ that can probe both core-collapse physics and the gravitational potential of our Galaxy.
  - Rotating radio transients (see McLaughlin et al. 2006)
  - Intermittent pulsars (see Kramer et al. 2006)
- Understanding the advanced stages of stellar evolution.
- Probing the interstellar medium of our Galaxy.
- Understanding the pulsar emission mechanism.

The aim of this paper is to investigate, for different configurations of the SKA and different computation power and data rates, a variety of different methods to achieve the best results for pulsar searches and pulsar timing. We approach this problem by using Monte Carlo simulations based on our current understanding of the Galactic pulsar population. In §2, we summarise the various configurations for the SKA. In §3, based on current population synthesis results, we investigate the SKA survey yields as a function of configuration and sky frequency. In §4, we describe a simple strategy for optimising follow-up timing observations. Computational requirements for the pulsar surveys are discussed in §5, from which we make specific recommendations in §6. Finally, in §7, we summarise our results.

2. SKA configurations

We will express different sensitivities as a fraction of one 'SKA unit' defined as $2 \times 10^4\,\mathrm{m^2\,K^{-1}}$. Following the preliminary specifications given by Schilizzi et al. (2007), we assume the SKA to consist of a sparse aperture array of tiled dipoles in the frequency range of 70 to 500 MHz and above 500 MHz it consists of one of the following three implementations:

A 3 000 15-m dishes with a single-pixel feed, a sensitivity of 0.6 SKA units, $T_{\rm sys}$=30 K and 70% efficiency covering the frequency range of 500 MHz to 10 GHz.

B 2 000 15-m dishes with phased array feeds from 500 MHz to 1.5 GHz, a sensitivity of 0.35 SKA units, a field of view (FoV) of $20\,\mathrm{deg^2}$, $T_{\rm sys}$=35 K and 70% efficiency and a single-pixel feed from 1.5 to 10 GHz, with $T_{\rm sys}$=30 K.

C A combination of a dense aperture array (AA) with a FoV of $250\,\mathrm{deg^2}$, a sensitivity of 0.5 SKA units, covering the frequency range of 500 to 800 MHz and 2 400 15-m dishes with a single-pixel feed covering the frequency range of 800 MHz to 10 GHz, a sensitivity of 0.5 SKA units, $T_{\rm sys}$=30 K and 70% efficiency.

We assume that 20% of the elements will be placed within a 1 km radius and 50% within a 5 km radius. The sparse aperture array below 500 MHz will be ignored, as we will not consider using it for pulsar surveys or timing in this paper. We will refer to the dishes from configurations A and B (which have a lower frequency limit of 500 MHz) as 500-MHz dishes and we will refer to the dishes from configuration C (which have a lower frequency limit of 800 MHz) as 800-MHz dishes.

3. Pulsar surveys

One of the main science goals for the SKA is to find the majority of the pulsar population in the Galaxy. These should include binary and millisecond pulsars, as well as transient and intermittent sources. A pulsar survey consists of two parts. The first part is using the telescope to observe parts of the sky with a certain dwell time. The total amount of telescope time depends on the FoV of the telescope, the chosen dwell time of the observation and the amount of sky that is searched. The second part is the analysis of the observations, which can be performed either real time, or off-line. Depending on the amount of data that needs to be analysed and especially if acceleration searches are employed to search for binary pulsars (see e.g. Lorimer & Kramer 2005), this can be a very computationally expensive task. Real time processing has been done in the past, but any major pulsar survey has always had an off line processing component (see e.g. Lorimer et al. 2006).

3.1. Technical considerations

The FoV of a survey has a maximum that depends on the characteristics of the elements used. In the case of circular dishes with a one pixel receiver, the FoV can be approximated as $(\lambda/D_{\rm dish})^2$ steradians, where λ is the wavelength at which the survey is undertaken and $D_{\rm dish}$ is the dish diameter. However, by placing a phased array feed at the focal point of the dish (see e.g. Ivashina et al. 2004), the FoV can be extended by a factor which we denote ξ. The total FoV then no longer depends on λ. In the case of the Aperture Array (AA), the FoV of the elements is about

half the sky. The actual size of the FoV that can be obtained will be limited by the available computational resources. This is because the signals from the elements will be combined coherently, resulting in 'pencil beams', the size of which scales with $1/D_{\rm el}^2$, where $D_{\rm el}$ is the distance between the furthest elements that are used in an observation. To obtain a large synthesised FoV it is therefore necessary to restrict the beam forming to using only the elements in the core of the telescope (so that $D_{\rm el} = D_{\rm core}$), which will, however, reduce the sensitivity.

3.2. Survey simulations

To find out how the SKA pulsar survey performance depends on different SKA configurations, we simulated SKA pulsar surveys for different collecting areas and different centre frequencies.

3.2.1. Simulation method

The simulations were performed following Lorimer et al. (2006) and using their Monte Carlo simulation package[1]. In their study, Lorimer et al. (2006) used the results from recent surveys with the Parkes Multibeam system to derive an underlying population of 30,000 normal pulsars with an optimal set of probability density functions (PDFs) for pulsar period (P), 1400-MHz radio luminosity (L), Galactocentric radius (R) and height above the Galactic plane (z). We make use of these results in our simulations described below which adopt the PDFs of model C' in Lorimer et al. (2006).

Our simulation procedure begins, following the findings of Lorimer et al. (2006), by generating 30 000 normal pulsars which beam towards the Earth. Each pulsar is assigned a value of P, L, R and z based on the assumed PDFs. Their initial positions in the plane of the Galaxy follow the spiral-arm modeling procedure described by Faucher-Giguère & Kaspi (2006). The intrinsic pulse width of each pulsar follows the power law relationship with spin period given in equation (5) of Lorimer et al. (2006) (see also their Figure 4). To compute the expected DM and scatter broadening effects on each pulse, we use the NE2001 electron density model (Cordes & Lazio 2002). Note that, since we are primarily concerned with the distant population of highly dispersed pulsars in these simulations, we do not attempt to account for interstellar scintillation. Finally, to allow us to extrapolate the 1400-MHz luminosities to other survey frequencies in the next step, we make the reasonable assumption that pulsar spectra can be approximated as a power law (Lorimer et al. 1995) and assign each pulsar a spectral index drawn from a normal distribution with mean of –1.6 and standard deviation 0.35. The same procedure was used to obtain a millisecond pulsar population, but with pulsar period and pulsar luminosity distributions from Cordes & Chernoff (1997) and assuming 30 000 potentially detectable millisecond pulsars in the Galaxy (Lyne et al. 1998).

Given the above model for the underlying population, which is consistent with the results of current-day surveys, we proceed to apply it to different configurations of the SKA. For each configuration, we compute the observed flux density of each pulsar and compare it with the limiting flux threshold, which depends on the sky temperature ($T_{\rm sky}$) and the observed width of the pulsar profile. For the AA we reduced the sensitivity by the cosine of the zenith angle of the source, as the AA is sensitive only to the component of the radiation projected onto the plane of the AA. In addition, because the core of the SKA will be located near a declination of –30°, the sky visible to the SKA was limited to a maximum declination of 50°.

As discussed by Lorimer et al. (2006), we make the important distinction between the observed (i.e. post-detection) pulse width which is related to the pulsar's intrinsic pulse width by the quadrature sum of contributions from sampling, dispersion smearing and scattering (see equation 4 of Lorimer et al. (2006)). To scale the scatter-broadening time to arbitrary SKA survey frequencies, we adopt a frequency power law index of –4 (Cordes & Lazio 2002). We consider a pulsar to be detected by a given configuration if its flux density exceeds the threshold value, and its observed pulse width is less than the spin period.

Initially, we determined the optimal centre frequencies for a survey in the Galactic plane (defined as $|{\rm l}| < 45°$ and $|{\rm b}| < 5°$) and an all-sky survey excluding the Galactic plane. This was done by comparing the detected number of normal pulsars by simulating surveys with sensitivities in the range 0.1 to 0.5 SKA units (in steps of 0.1 SKA units) and with centre frequencies in the range 0.4 to 2 GHz (in steps of 0.25 GHz). For each sensitivity and for both survey types, the frequency that provided the largest number of pulsars was chosen as the optimal frequency. To find the frequency that provided the largest number of pulsars, a cubic polynomial function was fitted through the points. The optimal centre frequencies for a pulsar survey inside and outside the Galactic plane are shown in Fig. 1. It can be seen that the optimal survey frequency decreases with lower sensitivity. The reason for this is that for lower sensitivity, the average distance to the detected pulsar is smaller. Thus, frequency dependent propagation effects are smaller, allowing lower frequencies to be used. It is surprising that the optimal centre frequencies for normal and millisecond pulsars are similar, since scattering effects on the pulsar profile have a larger impact on the detection of millisecond pulsars than on the detection of normal pulsars. Thus it can be expected that in the Galactic plane, higher observation frequencies would favour the detection of millisecond pulsars. However, millisecond pulsars have a steep luminosity distribution (e.g. Cordes & Chernoff 1997), leading to many low-luminosity millisecond pulsars which are not detected

[1] The package psrpop can be obtained from `http://psrpop.sourceforge.net`. Additional software to simulate and analyse a series of surveys can be obtained from: `http://www.jb.man.ac.uk/~rsmits/SKA.tgz`

at high observation frequencies. It should be noted that with 500 MHz bandwidth, the lowest centre frequency is 750 MHz for the 500-MHz dishes and 1.05 GHz for the 800-MHz dishes. Once the optimal centre frequencies were determined, these restrictions were included in the simulations. We then performed four simulations corresponding to possible pulsar surveys. For the dishes they were performed at the optimal centre frequencies, taking the frequency limits into account. The frequency range of the AA was held fixed at 500 to 800 MHz. The simulations are:

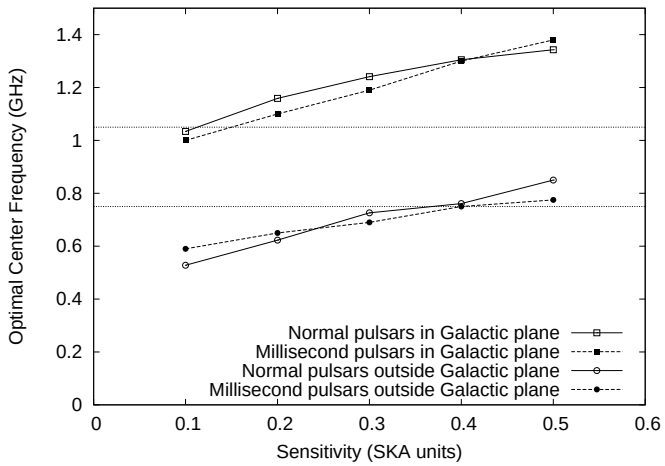

Fig. 1. Optimal frequency to survey the Galactic plane ($|b| < 5°$, $|l| < 45°$) or outside the Galactic plane ($|b| > 5°$, $|l| > 45°$) as a function of sensitivity. The dotted horizontal lines show the lowest available centre frequency of the 500-MHz (bottom line) and 800-MHz (top line) dishes. Surveys with the AA were performed at a centre frequency of 650 MHz.

- An all-sky survey with the AA (including the Galactic plane) and a Galactic plane survey with the 800-MHz dishes. This shows the fraction of pulsars that can be found with configuration C.
- An all-sky survey with just the AA. This shows the fraction of pulsars that will be found with configuration C, if we do not include the dishes in the survey.
- An all-sky survey with the 500-MHz dishes. This shows the fraction of pulsars that can be found with configurations A or B.
- A Galactic plane survey with the 500-MHz dishes. This shows the fraction of pulsars that will be found with configuration A or B, without performing a survey outside the Galactic plane.

We assumed a bandwidth of 500 MHz for the dishes and 300 MHz for the AA and an integration time of 1800 s. The simulations were limited to isolated pulsars only. A paper addressing the problems of the searching for and timing of binary pulsars is in preparation (Smits et al. in prep.)

A Galactic centre survey with the SKA will allow for testing the conditions near a $3 \times 10^6\,M_\odot$ black hole. Simulating such a survey requires a detailed modelling of the scattering in the Galactic centre. Previous work (e.g. Lazio & Cordes 1998; Bhat et al. 2004; Cordes et al. 2004) shows that frequencies above 10 GHz are required to penetrate the scattering screen surrounding the Galactic centre. These results can be used for a detailed study of a Galactic centre survey with the SKA. However, such a study is beyond the scope of this paper. Further results on this issue will be presented in J. Deneva et al. (in prep.)

3.2.2. Simulation results

Fig. 2 shows the fraction of normal and millisecond pulsars that were detected in the simulation of 4 different surveys as a function of sensitivity. Only 1.5% of the pulsars could not be detected due to the declination of the SKA of –30°. As will be shown in Section 5, we expect that initially only the 1-km core of the SKA can be used for the pulsar survey. This leads to a sensitivity of 0.1 SKA units, which is similar to having a fully steerable Arecibo-class telescope in the southern hemisphere. Performing an all-sky survey with only the 1-km core of the SKA, will detect about 14 000 normal pulsars out of a possible 30 000 and about 6 000 millisecond pulsars out of a possible 30 000, regardless of the SKA implementation. The total observation time of the survey, however, does depend on the implementation. Using single-pixel feed dishes to perform an all-sky survey or a survey of just the Galactic plane will take 600 days and 30 days, respectively. With phased array feed dishes or an AA the total survey time can be much less, depending on the available computation power (see Section 6). Because of the large natural FoV of the SKA and it's location in the southern hemisphere, the 1-km core of the SKA complements and extends work done by both Arecibo and the Five hundred meter Aperture Spherical Telescope (FAST), which is expected to be completed around 2014.

4. Timing

All pulsars that will be found by the SKA need to become part of a regular timing program to find the interesting pulsars. Ideally, they need to be timed once every two weeks for about 6 months to a signal-to-noise ratio of about 9 (which is only a nominal target to characterise the new pulsars and to identify those sources which are interesting for high precision timing)[2]. The minimum timing duration is also restricted by the pulsar stabilisation time, which is the time it takes to obtain a stable integrated profile. Assuming that they will be timed using dishes, the total duration of timing all newly discovered pulsars just once depends on how the observations are performed,

[2] Usually, at least 12 months are needed to break the degeneracies between positional uncertainties and pulsar spin-down. However, we assume that the imaging capabilities of the SKA will be used after the discovery to obtain an interferometric position, which speeds up the process.

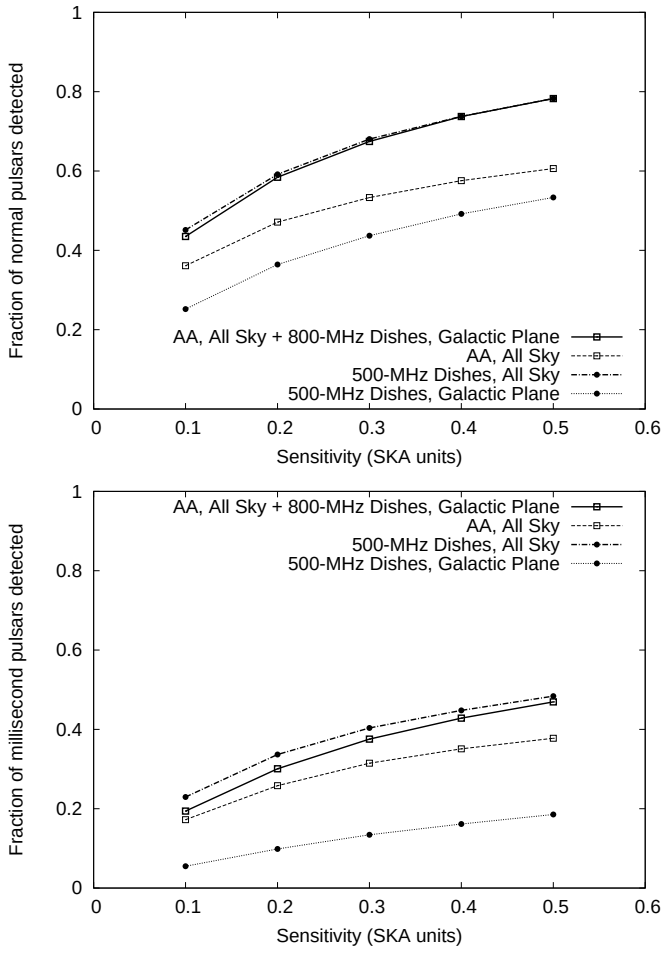

Fig. 2. Fraction of normal (top) and millisecond (bottom) pulsars detected from different pulsar survey simulations as a function of sensitivity of the SKA. For both the 500-MHz and 800-MHz dishes, the surveys were performed at the optimal centre frequency, taking the frequency limits into account (see Fig. 1). The frequency range of the AA was 500 to 800 MHz.

i.e. at which points on the sky the telescope is pointed. To estimate the total duration of this timing process, we therefore suggest the following scheme that minimises the average observation time per pointing, by grouping dim pulsars together in one FoV. Let $\rho_{\rm fov}$ be the angle of the FoV.

1. All pulsars are placed on a long list, in order of increasing brightness.
2. All pulsars within an angle of $\rho_{\rm fov}$ from the first pulsar of the list (the dimmest pulsar) are placed on a short list.
3. We now consider the dimmest pulsar on the short list. If possible, we restrict the pointing of the FOV to include this pulsar and we remove this pulsar from both the short list and the long list. If the pointing of the FOV is already too restricted to include this pulsar, it is removed from the short list only.
4. Step 3 is repeated until the short list is empty. The resulting pointing is stored.
5. Step 2 through 4 are repeated until the long list is empty.

This timing optimisation method saves about 30 to 50% of observation time over a simple grid approach. To compare timing performances, we used this scheme to estimate the time to obtain a single timing point of 14 000 pulsars from an all-sky survey to a signal-to-noise ratio of 9 for each of the SKA-configurations, assuming usage of the full collecting area and a pulsar stabilisation time (see e.g. Helfand et al. 1975) of 200 pulses. This leads to observation times of 6 days for configuration A and 1.5 days for both configurations B and C. For configuration C the AA was used to time all the pulsars that were detected by the AA in the survey. These estimates do not include densely spaced 'resolving' observations that are required to obtain the first phase coherent timing solution. Fig. 3 shows the simulated pulsar-sky and the pointings that result from the timing optimisation method, assuming the 20 deg^2 FoV of configuration B.

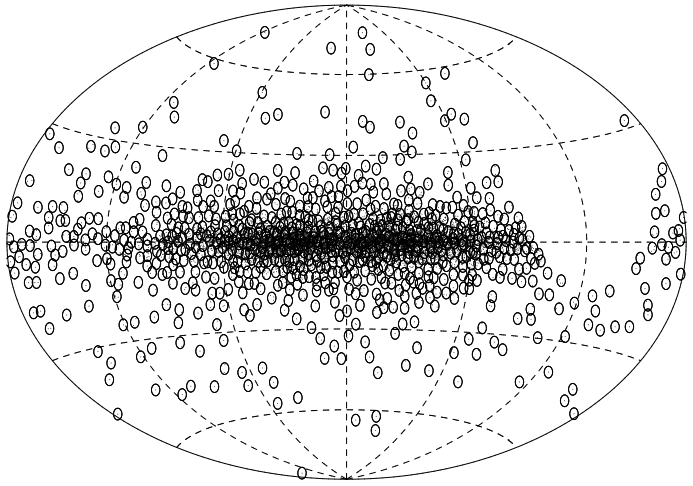

Fig. 3. Hammer projection of the Galaxy with 14 000 detected pulsars from an SKA pulsar survey simulation. The horizontal axis corresponds to longitude and the vertical axis corresponds to latitude. The Galactic centre is located in the middle of the plot. The dashed lines running from top to bottom correspond to steps of 60° in longitude, whereas the dashed lines running from left to right correspond to steps of 30° in latitude. The circles indicate all pointings (700) that result from the timing optimisation method, assuming a FoV of 20 deg^2.

To perform strong field tests of General Relativity and gravitational wave detection, as defined in the key science project, it is essential to time a large number of specific pulsars to signal-to-noise ratios of up to 100 on a regular basis. To estimate how much observation time is required for such high-precision timing, we have to distinguish between timing millisecond pulsars (for the Pulsar Timing Array) and timing pulsars in a binary with a neutron star

or a black hole companion. We calculated the observation time for timing the 250 millisecond pulsars with the best signal-to-noise ratio's for the three configurations. We assumed that for timing purposes, the nearly full collecting area (out to several hundreds of kilometres from the core) of the SKA can be used. As a conservative estimate (subject to current studies), we timed every pulsar for at least 5 minutes to ensure a stable pulsar profile to minimise the error in the time of arrival. With the single-pixel feed 15-m dishes this takes about 20 hours, the 15-m dishes with phased array feeds take about 15 hours and the AA only takes about 6 hours. However, this assumes that the polarisation purity after calibration of the AA is similar to that of the dishes, which might not be the case. To estimate the maximum required observation time for timing pulsars in a binary with a neutron star or black hole, we will assume a (somewhat optimistic) number of 200 such binaries that are potentially detectable in the Galaxy. We further assume that the characteristics of the pulsars in these binaries are similar to isolated pulsars. This leads to a detection of 90 compact binary pulsars. With the single-pixel feed 15-m dishes it takes about 2 days to time these binary pulsars, the 15-m dishes with phased array feeds take about 1.5 days and the AA only takes about 8 hours (once again, assuming similar polarisation purity as the dishes). However, timing only the brightest 80% of the binary pulsars, would take about half the observation time. It should be noted that these are only initial estimates to give an indication of the maximum required observation time for high-precision timing and to compare the performance of the different configurations. A paper containing a more detailed study on high-precision timing is in preparation (Smits et al. in prep.).

5. Computational requirements

A pulsar survey requires the coherent addition of the signals from the elements in the core of the SKA and to form sufficient pencil beams to create the required FoV. These pencil beams will produce a large amount of data which will need to be analysed. We estimate the required computation power and data rates for 3 000 15-m dishes with a bandwidth of 500 MHz and 2 polarisations and for the AA with a frequency range from 500 to 800 MHz and 2 polarisations.

5.1. Beam forming

Following Cordes (2007), we estimate the number of operations per second (ops), $N_{\rm osb}$, to fill the entire FoV of a dish with pencil beams as[3]:

$$N_{\rm osb} = F_c N_{\rm dish} N_{\rm pol} B \xi \left(\frac{D_{\rm core}}{D_{\rm dish}}\right)^2, \quad (1)$$

where F_c is the fraction of dishes inside the core, $N_{\rm dish}$ is the total number of dishes, $N_{\rm pol}$ is the number of polarisations, B is the bandwidth, $D_{\rm dish}$ is the diameter of the dishes, $D_{\rm core}$ is the diameter of the core and ξ is the factor by which the phased array feed extends the FoV. To fill the FoV of single-pixel 15-m dishes in a 1-km core requires 4 400 pencil beam. The number of operations per second to beam form a 1-km core containing 20% of 2 400 single-pixel 15-m dishes then becomes 2.2×10^{15}. The number of operations for beam forming the full FoV of 15-m dishes with a phased array feed are simply a factor ξ higher, corresponding to the increase in FoV. For the SKA implementation B, this corresponds to $\xi = 31$. The number of operations for beam forming can be reduced by beam forming in two stages, if we assume that the dishes in the core are positioned such that they can form sub-arrays that all have the same size. In the first stage, beam forming of the full FoV is performed for each sub-array. In the second stage the final pencil beams are formed by coherently adding the corresponding beams of each sub-array formed in the first stage. When the sub-arrays have the optimal size given by $D_{\rm core}(F_c N_{\rm dish})^{-1/4}$, as we show in the Appendix, the number of operations per second becomes

$$N_{\rm osb} = 2\sqrt{F_c N_{\rm dish}} N_{\rm pol} B \xi \left(\frac{D_{\rm core}}{D_{\rm dish}}\right)^2. \quad (2)$$

For the same parameters as above, the number of operations per second becomes 2.0×10^{14}. For the beam forming of the AA, the calculations are slightly different. Initial beam forming will be performed at the stations themselves, leading to beams equivalent to those of a 60-m dish for each station. Demanding a total FoV of 3 deg^2 and assuming a total collecting area of 500 000 m^2, the number of operations becomes:

$$N_{\rm osb} = F_c N_{\rm dish} N_{\rm pol} B \cdot 3 \left(\frac{\pi}{180 c}\right)^2 D_{\rm core}^2 \nu_{\rm max}^2, \quad (3)$$

where c is the speed of light and $N_{\rm dish} \approx 177$. For a 1-km core, this leads to a required computation power of 1.4×10^{14} ops. Fig. 4 shows the number of operations per second for the beam forming as a function of core diameter for the 15-m dishes with single-pixel feed and the AA. To obtain the benchmark concentration as a continuous

[3] Note that for a phased array feed this function is actually frequency dependent, because the total FoV of the dish then becomes constant, yet the FoV of the pencil beams is given by $(\lambda/D_{\rm tel})^2$. However, for the values of bandwidth and observation frequency used in this paper, Eq. 1 is accurate.

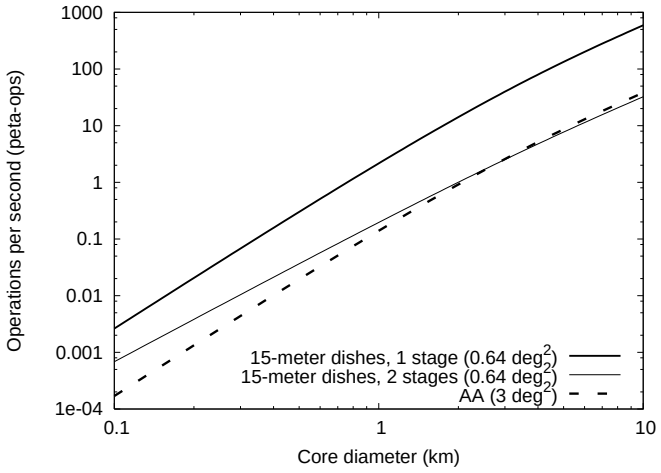

Fig. 4. The number of operations per second required to perform the beam forming for the 15-m dishes and the AA. It is assumed that there are 2 400 15-m dishes and the bandwidth is 500 MHz. The FoV of 0.64 deg^2 corresponds to filling the natural FoV of the dishes ($\xi = 1$) at a frequency of 1.4 GHz. For the AA we assume a FoV of 3 deg^2 and a total collecting area of 500 000 m^2. The frequency range is 0.5 to 0.8 GHz. In all cases the number of polarisations is 2. The thick black line corresponds to the beam forming of the 15-m dishes in one stage. The thin black line corresponds to the beam forming of the 15-m dishes in two stages. The striped/dotted line corresponds to the beam forming of the AA.

function of core diameter between 0 and 10 km, we used the following expression:

$$F_c(D_{\rm core}) = a[1 - \exp(-bD_{\rm core})], \quad (4)$$

where a and b were tuned to the specifications of 20% and 50% of the dishes within a 1-km and 5-km core, respectively, which leads to $a = 0.56$ and $b = 0.45 \times 10^{-3}\,{\rm m}^{-1}$.

As an alternative to beam forming by coherently adding the signals from the dishes up to a certain core size, it is also possible to perform the beam forming by incoherently adding the signals from sub-arrays. This process is similar to beam forming in two stages as mentioned above, except that in the second stage the beams that were formed in the first stage are added incoherently. This leads to a much larger beam size, which reduces the required computation power for beam forming significantly. It also reduces the total data rate and the required computation power for the data analysis. The drawback is that it reduces the sensitivity of the telescope by a factor of $\sqrt{N_{\rm sa}}$, where $N_{\rm sa}$ is the number of sub-arrays, which will be several hundred. However, this can be partially compensated as this method allows utilising all elements that are placed in sub-arrays of the same size, which can possibly be as much as 5 times the collecting area of the core of the SKA.

5.1.1. Data analysis

There are two factors which impact the total data volume to be analysed. Firstly, the FoV will be split up in many pencil beams, each of which will need to be searched for pulsar signals. Secondly, the SKA will be able to see the majority of the sky, all of which we want to search for pulsars and pulsar binaries. There are two ways to achieve this. The first option is to analyse the data as it is received, immediately discarding the raw data after analysis. This requires the analysis to take place in real time. The second option is to store all the data from part of the survey and analyse them at any pace that we see fit before continuing with the next part of the survey. Both approaches pose serious technical challenges, which we will discuss here.

First we consider the dishes for which we estimate the data rate of one pencil beam as

$$\mathcal{D}_{\rm dish} = \frac{1}{t_{\rm samp}} \frac{B}{\Delta\nu} N_{\rm pol} \frac{N_{\rm bits}}{8}\,{\rm Bps}, \quad (5)$$

where $t_{\rm samp}$ is the sampling time, B is the bandwidth, $\Delta\nu$ is the frequency channel width, $N_{\rm pol}$ is the number of polarisations and $N_{\rm bits}$ is the number of bits used in the digitisation. $\Delta\nu$ can be estimated by demanding that the dispersion smearing within the frequency channel does not exceed the sampling time, which leads to:

$$\Delta\nu({\rm GHz}) = \frac{t_{\rm samp}(\mu{\rm s})\nu^3_{\rm min}({\rm GHz})}{8.3 \times 10^3 {\rm DM}_{\rm max}}, \quad (6)$$

where $\nu_{\rm min}$ is the minimum (lowest) frequency in the observation frequency band and ${\rm DM}_{\rm max}$ is the maximum expected dispersion measure. For the dishes, the number of pencil beams to fill up the FoV can be estimated as $\xi(D_{\rm core}/D_{\rm dish})^2$. For the AA, the number of pencil beams becomes frequency dependent and for 3 deg^2 FoV it is given by

$$N_{\rm pbAA} = 3\left(\frac{\pi}{180c}\right)^2 D^2_{\rm core}\nu^2. \quad (7)$$

However, a pencil beam needs to be centred on the same point on the sky over the frequency band to allow for summing over frequency. Thus, even though the pencil beams become larger towards lower frequency, the number of pencil beams needs to remain constant and is determined by the highest frequency. The total data rate from the AA can then be estimated as

$$\mathcal{D}_{\rm AA} = \frac{1}{t_{\rm samp}} \frac{B}{\Delta\nu} N_{\rm pol} \frac{N_{\rm bits}}{8} 3\left(\frac{\pi}{180c}\right)^2 D^2_{\rm core}\nu^2_{\rm max}\,{\rm Bps}. \quad (8)$$

Fig. 5 shows the data rate from a pulsar survey for the 15-m dishes and the AA as a function of core diameter, assuming $t_{\rm samp}$=100 μs, ${\rm DM}_{\rm max}$=1000 cm^{-3} pc for the dishes and ${\rm DM}_{\rm max}$=500 cm^{-3} pc for the AA, $N_{\rm pol}$=1 (sum of 2 polarisations) and 2 bit digitisation. The AA was assumed to operate on the full frequency range of 0.5 to 0.8 GHz. The frequency range for the dishes was assumed to be 1 to 1.5 GHz. For a 1-km core, the data rate for the 15-m dishes with single-pixel feed is 4.7×10^{11} bytes per

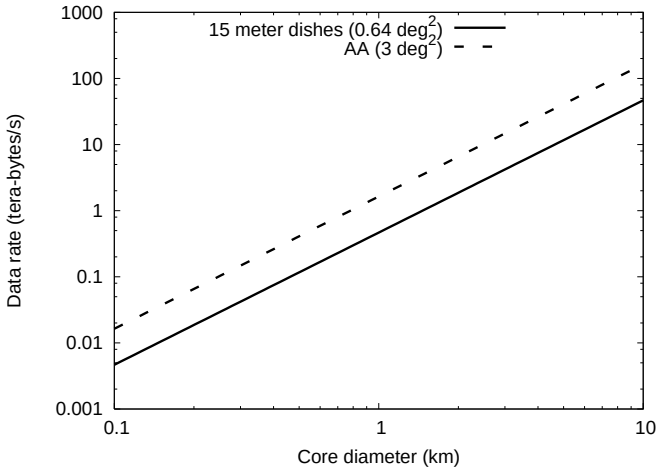

Fig. 5. Data rate from pulsar surveys using the 15-m dishes or the AA, as a function of core diameter.

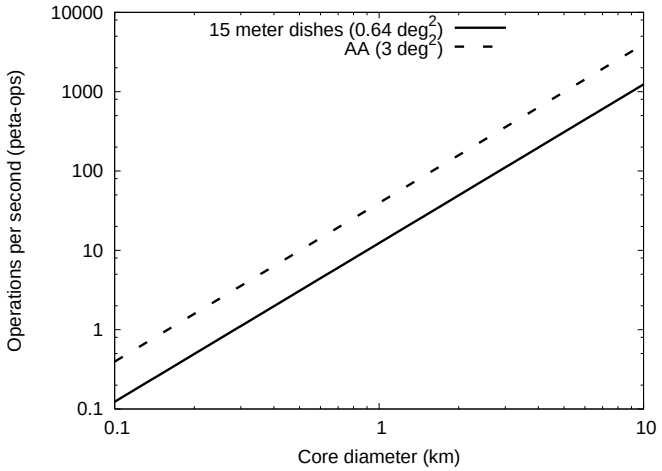

Fig. 6. Operations per second required to perform a real time analysis of pulsar surveys using the 15-m dishes or the AA, as a function of core diameter.

second and for the AA it is 1.6×10^{12} bytes per second. Both values scale linearly with the FoV. We can estimate the number of operations to search one 'pencil beam' for accelerated periodic sources as one Fourier Transform of all the samples in the observation, for each trial DM-value and for each trial acceleration:

$$N_{\rm oa} = N_{\rm DM} N_{\rm acc} \times 5 N_{\rm samp} \log_2(N_{\rm samp}), \quad (9)$$

where $N_{\rm DM}$ is the number of trial DM-values, $N_{\rm acc}$ is the number of trial accelerations which scales with the square of $N_{\rm samp}$, which is the number of samples in one observation. Thus, the number of operations for the analysis scales as $N_{\rm samp}^3 \log(N_{\rm samp})$. This means that increasing the observation length is computationally very expensive. Once again, for the dishes the number of pencil beams to fill up the FoV can be estimated as $\xi(D_{\rm core}/D_{\rm dish})^2$ and for the AA the number of pencil beams is given by Eq. 7, with ν=$\nu_{\rm max}$=0.8 GHz. Fig. 6 shows the number of operations per second required to perform a real time analysis of a pulsar survey with the 15-m dishes and the AA as a function of core diameter, assuming 100 trial accelerations, a sampling time of 100 μs and an observation time of 1 800 s. $N_{\rm DM}$ was taken to be equal to the time shift due to the maximum dispersion divided by the sampling time, which is equal to

$$N_{\rm DM} = \frac{4150 DM_{\rm max}(\nu_{\rm min}^{-2}({\rm GHz}) - \nu_{\rm max}^{-2}({\rm GHz}))}{t_{\rm samp}(\mu{\rm s})}. \quad (10)$$

For a 1-km core, the required computation power becomes $1.2{\times}10^{16}$ and $4.0{\times}10^{16}$ ops for the 15-m dishes and the AA, respectively. These values are lower estimates of the actual number of operations, as there will be significant contributions from dedispersion, harmonic folding and possibly other processes that will contribute to the total number of operations. These additional processes are all on the order of $N_{\rm samp}$ and we expect their total contribution to be similar to one Fourier Transform at most.

Alternatively, we can consider storing the data from a part of the survey and analyse it at a much slower rate

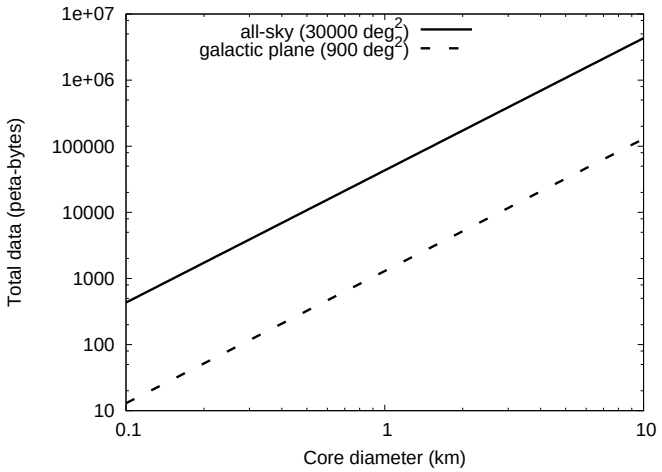

Fig. 7. Total amount of data from an all-sky survey (35 000 deg^2) and a survey of the Galactic plane (900 deg^2) as a function of core diameter, assuming a frequency range of 1 to 1.5 GHz. A 1-km core would correspond to 20% of the collecting area of the SKA.

(see further discussion in Section 6.2). From Eq. 5 we can estimate the total amount of data from a survey. Fig. 7 shows the total amount of data from an all-sky survey and a survey of the Galactic plane as a function of core diameter, assuming a frequency range of 1 to 1.5 GHz, $t_{\rm samp}$=100 μs, DM$_{\rm max}$=1000 cm^{-3} pc, $N_{\rm pol}$=1, an observation time of 1 800 s and 2 bits digitisation. Assuming a storage capacity of 1 exa-byte, an all sky survey would have to be split up in about 40 parts. The total time of the survey would then depend on the speed at which the analysis takes place.

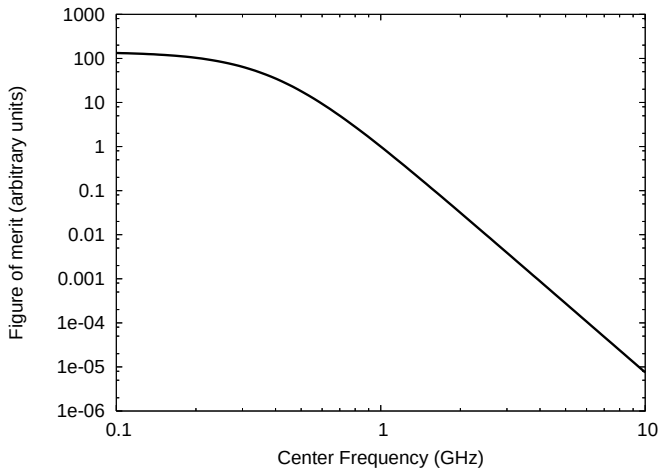

Fig. 8. The frequency dependence of the figure of merit. This function expresses the speed of the survey for a fixed sensitivity of the telescope.

5.1.2. Survey speed

To express the trade-off between the SKA design and survey speed, we define the figure of merit for dishes as (see appendix for derivation)

$$M = \eta\xi B \left(\frac{N_{\rm dish} D_{\rm dish}}{T_{\rm tel} + T_{\rm sky}^{400} \left(\frac{\nu}{400\,{\rm MHz}}\right)^{-2.6}} \right)^2 \nu^{2\alpha-2}, \qquad (11)$$

where η is the aperture efficiency, ξ is the factor by which the phased array feed extends the FoV, B is the bandwidth, $N_{\rm dish}$ is the number of dishes used in the survey, $D_{\rm dish}$ is the diameter of the dish, $T_{\rm tel}$ is the system temperature of the telescope (K), $T_{\rm sky}^{400}$ is the sky temperature (K) at 400 MHz ($T_{\rm sky}$ scales as $\nu^{-2.6}$), ν is the observation frequency, and α is the average spectral index of radio pulsars, which is about –1.6 (Lorimer et al. 1995). The figure of merit shown here expresses the speed of the survey for a required sensitivity of the telescope and is identical to that for a continuum survey of steady sources. It does not include the loss of sensitivity associated with pulse broadening effects and does not express the impact of dedispersion and periodicity search on the survey time.

Fig. 8 shows the strong dependence of the figure of merit on the observation frequency. The slope at high frequencies is due to the spectral index of pulsars and the decrease of the FoV. At low frequency the figure of merit becomes flat as the sky temperature begins to dominate the system temperature. In practise, pulsars become harder to detect at low frequencies where scattering effects broaden the pulsar profile. Since the scattering depends on the location on the sky, it was not included in the merit function. Thus, at low frequencies the figure of merit is overestimated. However, scattering effects are only significant for pulsars located in the Galactic plane. For non-millisecond pulsars, low frequencies are very favourable (see van Leeuwen & Stappers 2008).

The total observation time of a survey is given by:

$$t_{\rm total} = \frac{\Omega_{\rm sur}}{\Omega_{\rm FoV}} t_{\rm point} \qquad (12)$$

where $\Omega_{\rm sur}$ is the total solid angle of sky covered by the survey, $\Omega_{\rm FoV}$ is the total FoV of the dishes and $t_{\rm point}$ is the observation time per pointing.

6. Suggestions

An estimate of the computational power by 2015 is given by Cornwell (2005) to be 10 Pflop for $100 M. To estimate what the SKA can achieve for pulsar searches and timing, we will assume that several 10^{16} ops are available for beam forming and data analysis when this survey will be performed, which will be after 2020.

We consider three scenarios, two with full coherent beam forming, where the analysis takes place either in real time or off-line and one scenario where part of the beam forming takes place incoherently.

6.1. Real time analysis

First we assume that the analysis takes place real time. The immediate benefits are that no time is lost for the data analysis and that only reduced data needs to be stored. One drawback, however, is that the data can only be processed once. Experience with current pulsar surveys show that it is extremely advantageous to have multiple passes at pulsar survey data analysis (see e.g. Faulkner et al. 2005).

As calculated in Section 5.1.1, for a 1-km core the data rate from the dishes with a single-pixel feed is 4.7×10^{11} bytes/s. The required computational power for real time analysis is 1.2×10^{16} ops. Both values scale linearly with FoV. Only with SKA implementation B, where the dishes have phased array feeds, can the FoV of the dishes be increased beyond 0.64 deg^2. Using the 1-km core of the AA and using a FoV of 3 deg^2 leads to a data rate of 1.6×10^{12} bytes/s and requires a computation power of 4.0×10^{16} ops to analyse the data in real time.

SKA implementation A suggests the all-sky survey to be performed with single-pixel 15-m dishes. At low frequencies the FoV of the dishes is about 1 deg^2. The entire survey will then take about 600 days. (This value assumes 100% telescope time. In practice this survey might take up to 5 years to perform). In implementation B a larger FoV can be used. The survey time of 600 days then scales inversely with the FoV, however the data rates and required computation power go up linearly with the FoV. Implementation C has the benefit of the AA for which an all-sky survey takes only about 200 days and the survey of the Galactic plane with single-pixel 15-m dishes takes about 30 days. The data rates and required computation power for the AA are larger than for the dishes. When we take this into account the total survey time for all implementations become similar, except that implementations B and C allow for a faster survey and the AA in

implementation C might be used for other observations simultaneously (see Cordes 2007, for using the SKA as a synoptic survey telescope).

6.2. Off-line analysis

The off-line analysis requires the full data from an observation to be stored. Thus, the data rates from Fig. 5 become the rates at which data is written to a storage device. When the maximum data storage has been reached, the observation can be stopped and the data analysis can be performed at any pace suitable. After the data analysis has been completed, the next observation can be run. This allows a trade-off between computation cost and survey speed. A drawback is that, depending on available future storage solutions, the total survey time may easily become more than a decade for any SKA implementation.

6.3. Incoherent beam forming

For real time analysis, restrictions on the computational power and data rate will likely limit the FoV to about $3\,\mathrm{deg}^2$. The survey time will then become at least 200 days. Off-line analysis requires the huge data rates to be written to a storage device and will increase the survey time by a significant factor. We therefore consider the possibility of incoherent addition of the sub arrays, as described in Section 5.1.

We will assume that all the elements in the SKA are placed such that their signals can be combined to form sub-arrays (or stations in the case of the AA) of 60 metres in diameter (similar to van Leeuwen & Stappers 2008, for LOFAR). The pencil beams that are formed by coherently adding the signals from the sub-array elements are about 17 times larger than the pencil beams from coherently beam forming the 1-km core. Thus the number of pencil beams required to fill the FoV becomes about 280 times smaller. The computational requirements for beam forming, data analysis as well as the data rates go down linearly by this factor. This method of beam forming utilises the full collecting area of the SKA, which increases the sensitivity by a factor of 5. However, because the sub-arrays are added incoherently, the sensitivity decreases by the square root of the number of sub-arrays. For the AA there will be about 180 stations. Thus the sensitivity goes down by a factor of $\sqrt{180}/5 \approx 2.7$. Assuming that the dishes are placed in sub-arrays with a 20% filling factor, the number of sub-arrays will be between 600 and 900, depending on the SKA implementation. For incoherent beam forming the sensitivity will then go down by a factor between 5 and 6. Applying this to an all-sky survey leads to a detection of about 20% of all the detectable pulsars.

7. Summary

We have investigated the pulsar yields for different SKA configurations by simulating SKA pulsar surveys for different collecting areas and centre frequencies. For the Galactic plane, the optimal centre frequency lies just above 1 GHz. Outside the Galactic plane the optimal centre frequency lies between 600 and 900 MHz, depending on the collecting area. Combining the dishes and the AA to perform a survey inside the Galactic plane and outside the Galactic plane, respectively, would result in detection of roughly 14 000 normal pulsars and 6 000 millisecond pulsars. As Fig. 2 shows, increasing the collecting area within the 1-km core would improve the detected number of pulsars significantly. The number of detected pulsars scales roughly as $F_c^{0.4}$, where F_c is the fraction of collecting area in the core.

We also describe a simple strategy for follow-up timing observations and find that, depending on the configuration, it would take 1–6 days to obtain a single timing point for 14 000 normal pulsars. Configuration C, containing the AA, will be of great benefit here. Obtaining a single timing point for the high-precision timing projects of the SKA, will take less than 14 hours, 2 days, or 3 days, depending on the configuration. Once again, the presence of the AA allows for the fastest timing. In the case of high-precision timing, however, this assumes that the polarisation purity of the AA is similar to that of the dishes.

Performing a pulsar survey with the SKA requires the coherent addition of the signals of the individual elements, forming sufficient pencil beams as to fill the entire FoV of a single dish. Because of the extreme computational requirements that arise due to large baselines, it is not possible to combine the signals of all of the elements in the SKA. Rather, only the core of the SKA can be used for a pulsar survey. We have derived the computational requirements to perform such beam forming as a function of core-diameter for the 15-m dishes and the AA. For a 1-km core the requirements are 2.2×10^{15} and 1.4×10^{14} ops for the 15-m dishes and the AA, respectively. When the dishes are placed such that they can form sub-arrays, the computational requirement for beam forming goes down significantly. We have also calculated the data rates and the computational requirements for applying a search-algorithm to the data to find binary pulsars. Both limit the usage of the SKA for pulsar searches to a core of about 1 km.

Acknowledgements. The authors would like to thank Simon Johnston and Andrew Lyne for their useful suggestions and the referee, Scott Ransom, for his useful suggestions and comments. This effort/activity is supported by the European Community Framework Programme 6, Square Kilometre Array Design Studies (SKADS), contract no 011938. DRL is supported by a Research Challenge Grant from West Virginia EPSCoR. Research at Cornell University was supported by NSF Grant AST0507747.

Appendix

Beam forming of the dishes

Cordes (2007) estimated the number of operations to perform the beam forming for a pulsar survey as one operation (corre-

sponding to the phase shift of one element) for each dish and each polarisation at the Nyquist frequency. This needs to be performed for each of the pencil beams that fill the total FoV. This leads to the total number of operations per second

$$N_{\rm osb} = F_c N_{\rm dish} N_{\rm pol} B \left(\frac{D_{\rm core}}{D_{\rm dish}}\right)^2, \quad (13)$$

where F_c is the fraction of dishes inside the core, $N_{\rm dish}$ is the total number of dishes, $N_{\rm pol}$ is the number of polarisations, B is the bandwidth, $D_{\rm dish}$ is the diameter of the dishes and $D_{\rm core}$ is the diameter of the core. The fraction $(D_{\rm core}/D_{\rm dish})^2$ is equal to the required number of pencil beams to fill up the FoV. If we assume that the dishes in the core are positioned such that they can form sub-arrays, beam forming can take place in two stages. In the first stage beam forming of the full FoV is performed for each sub-array. In the second stage the final pencil beams are formed by coherently adding the corresponding beams of each sub-array formed in the first stage. This leads to the following expression for the number of operations required for beam forming in two stages:

$$\begin{aligned} N_{\rm osb2} &= N_{\rm sa} N_{\rm dishsa} N_{\rm pol} B \left(\frac{D_{\rm sa}}{D_{\rm dish}}\right)^2 \\ &\quad + \left(\frac{D_{\rm sa}}{D_{\rm dish}}\right)^2 N_{\rm sa} N_{\rm pol} B \left(\frac{D_{\rm core}}{D_{\rm sa}}\right)^2, \end{aligned} \quad (14)$$

where $N_{\rm sa}$ is the number of sub-arrays in the core, $N_{\rm dishsa}$ is the number of dishes in one sub-array and $D_{\rm sa}$ is the diameter of the sub-arrays. Substituting $N_{\rm dishsa} = F_c N_{\rm dish}/N_{\rm sa}$ and $N_{\rm sa} = (D_{\rm core}/D_{\rm sa})^2$ yields

$$\begin{aligned} N_{\rm osb2} &= F_c N_{\rm dish} N_{\rm pol} B \left(\frac{D_{\rm sa}}{D_{\rm dish}}\right)^2 \\ &\quad + N_{\rm pol} B \left(\frac{D_{\rm core}}{D_{\rm dish}}\right)^2 \left(\frac{D_{\rm core}}{D_{\rm sa}}\right)^2, \end{aligned} \quad (15)$$

which has a minimum at $D_{\rm sa} = D_{\rm core}(F_c N_{\rm dish})^{-1/4}$. At this minimum, the number of operations for beam forming in 2 stages is:

$$N^{\rm min}_{\rm osb2} = 2\sqrt{F_c N_{\rm dish}} N_{\rm pol} B \left(\frac{D_{\rm core}}{D_{\rm dish}}\right)^2. \quad (16)$$

Beam forming of the AA

For the AA, initial beam forming will be performed at each station; this will lead to beams equivalent to those of a 60-m dish. Assuming a collecting area of 500 000 m^2, this leads to about 177 stations. The FoV of 1 pencil beam is given by $(\lambda/D_{\rm Core})^2 = (c/\nu D_{\rm core})^2$ steradians, where c is the speed of light. Thus, to cover 3 deg^2 the required number of pencil beams is $(3\pi/180)^2/(c/\nu D_{\rm core})^2$. Within the frequency band, the number of pencil beams needs to remain identical as to enable summing over frequency. In order to have a full coverage of the 3 deg^2, the required number of pencil beams is therefore obtained by setting ν to $\nu_{\rm max}$. The number of operations per second to perform the beam forming of the AA is then given by (see also Eq. 3)

$$N_{\rm osb} = F_c N_{\rm dish} N_{\rm pol} B \cdot 3 \left(\frac{\pi}{180c}\right)^2 D^2_{\rm core} \nu^2_{\rm max}. \quad (17)$$

Derivation of figure of merit

Neglecting numerical factors and physical constants, the figure of merit expresses the speed of a survey for a given sensitivity of the telescope. It therefore scales with aperture efficiency (η), the FoV, the bandwidth (B), the square of the collecting area (A) and the reciprocal of the square of the system temperature ($T_{\rm sys}$). For a pulsar survey it also scales with the square of the flux of pulsars, which scales as ν^α, with ν the observation frequency and α the average spectral index of radio pulsars, which is about –1.6. Thus:

$$M = \eta B {\rm FoV} \left(\frac{A\nu^\alpha}{T_{\rm sys}}\right)^2. \quad (18)$$

The FoV is given by $\xi(\lambda D^{-1}_{\rm dish})^2$, where ξ is the factor by which the phased array feed extends the FoV and $D_{\rm dish}$ is the diameter of the antennas. This is equal to $\xi(c\nu^{-1}D^{-1}_{\rm dish})^2$. The collecting area can be expressed as $A = N_{\rm dish}\pi D^2_{\rm dish}/4$, where $N_{\rm dish}$ is the number of dishes used in the survey. $T_{\rm sys}$ is the sum of the telescope temperature and the sky temperature, the latter scaling with frequency as $\nu^{-2.6}$. Putting all this in Eq. 18 and removing all constants, yields:

$$M = \eta\xi B \left(\frac{N_{\rm dish} D_{\rm dish}}{T_{\rm tel} + T^{400}_{\rm sky}\left(\frac{\nu}{400\,{\rm MHz}}\right)^{-2.6}}\right)^2 \nu^{2\alpha-2} \quad (19)$$

Glossary

The following list summarises the meaning of the most important parameters in this paper.

- $T_{\rm sys}$: system temperature (including contributions from receiver and sky background.
- $T^{400}_{\rm sky}$: sky temperature at 400 MHz.
- FoV: Field of view, size of the sky area instantaneously covered by the telescope.
- η: aperture efficiency for dishes.
- $D_{\rm dish}$: diameter of a single dish.
- $D_{\rm el}$: distance between the furthest elements that are used in an observation. For any pulsar survey in this paper this parameter is equal to $D_{\rm core}$.
- $D_{\rm core}$: diameter of the core region.
- $N_{\rm osb}$: number of operations per second required for beam forming.
- $N_{\rm dish}$: total number of dishes.
- F_c: fraction of the number of dishes inside the core.
- $N_{\rm pol}$: number of polarisations.
- B: observing bandwidth.
- ξ: factor by which the phased array feed expands the FoV. Note that for a phased array feed this factor is frequency dependent.
- $\nu_{\rm max}$: maximum observing frequency.
- a, b: parameters appearing in Eq. 4.
- $\mathcal{D}_{\rm dish}$: survey data rate for one pencil beam.
- $\mathcal{D}_{\rm AA}$: total survey data rate for AAs.
- $t_{\rm samp}$: sampling time for pulsar survey.
- $\Delta\nu$: channel bandwidth for pulsar survey.
- $N_{\rm bits}$: number of bits used for digitisation of survey data.
- $\nu_{\rm min}$: lowest frequency used for pulsar survey.
- $DM_{\rm max}$: maximum dispersion measure to be searched or expected.
- $N_{\rm DM}$: number of trial DM-values.
- $N_{\rm samp}$: number of samples in each survey time series.

$N_{\rm acc}$: number of trial accelerations to be searched.
$N_{\rm pbAA}$: number of pencil beams for AAs.
$N_{\rm oa}$: number of operations to search one pencil beam in acceleration searches.
M: survey-speed figure-of-merit for searches with dishes.
$t_{\rm total}$: total observing time for a survey.
$t_{\rm point}$: observing time per survey pointing.
$\Omega_{\rm sur}$: total sky (solid angle) for survey.
$\Omega_{\rm FoV}$: total FoV for dishes.

References

Bhat, N. D. R., Cordes, J. M., Camilo, F., Nice, D. J., & Lorimer, D. R. 2004, ApJ, 605, 759
Cordes, J. 2007, SKA memo 97, http://www.skatelescope.org/PDF/memos/97_memo_Cordes.pdf
Cordes, J. M. & Chernoff, D. F. 1997, ApJ, 482, 971
Cordes, J. M., Kramer, M., Lazio, T. J. W., et al. 2004, New Astronomy Review, 48, 1413
Cordes, J. M. & Lazio, T. J. W. 2002, ArXiv Astrophysics e-prints
Cornwell, T. J. 2005, SKA memo 64
Faucher-Giguère, C.-A. & Kaspi, V. M. 2006, ApJ, 643, 332
Faulkner, A. J., Kramer, M., Lyne, A. G., et al. 2005, ApJ, 618, L119
Helfand, D. J., Manchester, R. N., & Taylor, J. H. 1975, ApJ, 198, 661
Hulse, R. A. & Taylor, J. H. 1975, 201, L55
Ivashina, M. V., bij de Vaate, J. G., Braun, R., & Bregman, J. D. 2004, in Presented at the Society of Photo-Optical Instrumentation Engineers (SPIE) Conference, Vol. 5489, Ground-based Telescopes. Edited by Oschmann, Jacobus M., Jr. Proceedings of the SPIE, Volume 5489, pp. 1127-1138 (2004)., ed. J. M. Oschmann, Jr., 1127–1138
Kramer, M., Backer, D. C., Cordes, J. M., et al. 2004, New Astronomy Review, 48, 993
Kramer, M., Lyne, A. G., O'Brien, J. T., Jordan, C. A., & Lorimer, D. R. 2006, Science, 312, 549
Lazio, T. J. W. & Cordes, J. M. 1998, ApJ, 505, 715
Lorimer, D. R., Faulkner, A. J., Lyne, A. G., et al. 2006, MNRAS, 372, 777
Lorimer, D. R. & Kramer, M. 2005, Handbook of Pulsar Astronomy (Cambridge University Press)
Lorimer, D. R., Yates, J. A., Lyne, A. G., & Gould, D. M. 1995, MNRAS, 273, 411
Lyne, A. G., Manchester, R. N., Lorimer, D. R., et al. 1998, MNRAS, 295, 743
McLaughlin, M. A., Lyne, A. G., Lorimer, D. R., et al. 2006, 439, 817
Schilizzi, R. T., Alexander, P., Cordes, J. M., et al. 2007, SKA draft, http://www.skatelescope.org/PDF/Preliminary Specifications of the Square Kilometre Array_v2.7.1.pdf
Terzian, Y. & Lazio, J. 2006, in Presented at the Society of Photo-Optical Instrumentation Engineers (SPIE) Conference, Vol. 6267, Ground-based and Airborne Telescopes. Edited by Stepp, Larry M.. Proceedings of the SPIE, Volume 6267, pp. 62672D (2006).
van Leeuwen, J. & Stappers, B. 2008, in American Institute of Physics Conference Series, Vol. 983, American Institute of Physics Conference Series, 598–600